Available online at www.sciencedirect.com
ScienceDirect
International Journal of Heat and Mass Transfer 51 (2008) 104–110
International Journal of HEAT and MASS TRANSFER
www.elsevier.com/locate/ijhmt

Study of MHD boundary layer flow over a heated stretching sheet with variable viscosity: A numerical reinvestigation

Asterios Pantokratoras

School of Engineering, Democritus University of Thrace, 67100 Xanthi, Greece

Received 30 September 2005
Available online 4 June 2007

Abstract

This work is a critique to a paper published in the International Journal of Heat and Mass Transfer 48 (2005) 4460–4466, which concerns the boundary layer flow of an electrically conducting incompressible fluid over a heated stretching sheet. The flow is permeated by a uniform transverse magnetic field and the fluid viscosity is assumed to vary as a linear function of temperature. In the published paper the calculation domain was small and the temperature profiles are truncated. Although the dynamic viscosity has been considered a function of temperature and consequently variable inside the boundary layer the Prandtl number, which depends on viscosity, has been considered constant inside the boundary layer. The results of the present work are obtained with the direct numerical solution of the boundary layer equations taking into account both viscosity and Prandtl number variation across the boundary layer. The temperature profiles of the present work are quite different from those of the above work.

Keywords: MHD flow; Temperature-dependent viscosity; Variable Prandtl number

1. Introduction

The problem of forced convection along an isothermal constantly moving plate is a classical problem of fluid mechanics that has been solved for the first time in 1961 by Sakiadis [2]. Thereafter, many solutions have been obtained for different aspects of this class of boundary layer problems. Mukhopadhyay et al. [1] in a recent paper treated the MHD problem along a linearly stretching sheet considering that the fluid viscosity varies as a linear function of temperature. The authors applied a very interesting scaling group of transformations to the governing equations and after finding two absolute invariants they derived a third order ordinary differential equation corresponding to momentum equation and a second order ordinary differential equation corresponding to energy equation. Afterwards the equations were solved numerically. However in this paper there is an omission and two disadvantages. The omission is that the presented method has not been validated with comparison to existing results. This led to the first disadvantage that all the presented temperature profiles are wrong. The authors treated in a suitable manner the variation of viscosity with temperature in the momentum equation but this has not been done in the energy equation and this is the second disadvantage. For these reasons we resolved the above problem with the direct numerical solution of the boundary layer equations without any transformation. Our arguments will be confirmed below.

2. The mathematical model

Consider laminar flow along a flat plate with u and v denoting, respectively, the velocity components in the x and y direction, where x is along the plate and y is the coordinate perpendicular to x. For steady, two-dimensional flow the equations including variable viscosity are [1]

E-mail address: apantokr@civil.duth.gr

0017-9310/$ - see front matter © 2007 Elsevier Ltd. All rights reserved.
doi:10.1016/j.ijheatmasstransfer.2007.04.007

Nomenclature

B_o	strength of magnetic field
f	stream function
M	Hartmann number
Pr	Prandtl number
Re_x	Reynolds number
T	temperature
u	horizontal velocity
v	vertical velocity
x	horizontal coordinate
y	vertical coordinate

Greek symbols

η	similarity variable
θ	dimensionless temperature
κ	thermal diffusivity
μ	dynamic viscosity
ν	kinematic viscosity
ρ	density
σ	electrical conductivity

Subscripts

a	ambient
w	wall

Continuity equation:

$$\frac{\partial u}{\partial x}+\frac{\partial v}{\partial y}=0 \tag{1}$$

Momentum equation:

$$u\frac{\partial u}{\partial x}+v\frac{\partial v}{\partial y}=\frac{1}{\rho}\frac{\partial}{\partial y}\left(\mu\frac{\partial u}{\partial y}\right)-\frac{\sigma B_0^2}{\rho}u \tag{2}$$

Energy equation:

$$u\frac{\partial T}{\partial x}+v\frac{\partial T}{\partial y}=\kappa\frac{\partial^2 T}{\partial y^2} \tag{3}$$

where ρ is the fluid density (assumed constant), μ is the fluid dynamic viscosity, σ is conductivity of the fluid, B_o is the strength of the magnetic field, T is the fluid temperature and κ is the fluid thermal diffusivity. The boundary conditions are as follows:

$$\text{at } y=0 \quad u=u_w=cx, \quad v=0, \quad T=T_w \tag{4}$$

$$\text{as } y\to\infty \quad u\to 0, \quad T\to T_a \tag{5}$$

where c is a constant and T_a is the ambient medium temperature.

The dynamic viscosity is assumed to be a linear function of temperature given by the following equation [1]:

$$\mu=\mu_a[a+b(T_w-T)] \tag{6}$$

where μ_a is the ambient fluid dynamic viscosity and a and b are constants.

Eqs. (1)–(3) represent a two-dimensional parabolic flow. Such a flow has a predominant velocity in the streamwise coordinate (unidirectional flow) which in our case is the direction along the plate. The equations were solved directly, without any transformation, using the finite difference method of Patankar [3]. The solution procedure starts with a known distribution of velocity and temperature at the plate edge ($x=0$) and marches along the plate. At the leading edge the temperature was taken uniform and equal to ambient one and the velocity was also uniform with a very small value. At each downstream position the discretized equations are solved using the tridiagonal matrix algorithm (TDMA). The cross-stream velocities v were obtained from the continuity equation. The forward step size Δx was 0.001 mm and we used a nonuniform lateral grid with 500 points where Δy increases along y. In the numerical solution of the boundary layer problems the calculation domain must always be at least equal or wider than the boundary layer thickness. However, it is known that the boundary layer thickness increases with x. Therefore, it would be desirable to have a grid which conforms to the actual shape of the boundary layer. For that reason the calculation domain must always be at least equal or wider than the boundary layer thickness. In this work an expanding grid has been used (Fig. 1) according to the following equation:

$$y_{out}=y_o+cx \tag{7}$$

where y_{out} is the outer boundary of the calculation domain, c is the spreading rate of the outer boundary and x is the distance at the current step. In each case we tried to have a calculation domain wider than the real boundary layer

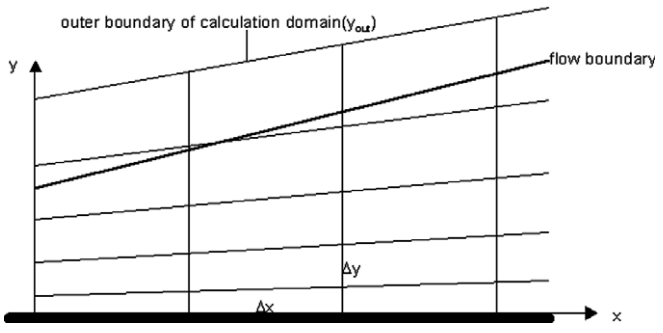

Fig. 1. The flow configuration and coordinate system.

thickness. This has been done by trial and error. If the calculation domain was thin the velocity and temperature profiles were truncated. In this case we used another wider calculation domain in order to capture the entire velocity and temperature profiles. This has been done by changing the coefficient c in Eq. (7). An analogue iterative procedure has been used by Cortell [4,5] to obtain temperature and velocity profiles along a stretching sheet. The technique used by Cortell was applied to the transformed equations.

The results are grid independent. The parabolic solution procedure is a well known solution method and has been used extensively in the literature. It appeared for the first time in 1970 [6] and has been included in classical fluid mechanics textbooks (see p. 275 in White [7]). Anderson et al. [8] mention seven numerical methods for the solution of the boundary layer equations (p. 364) and among them is the "well known Patankar–Spalding method". The method is fully implicit and can be applied to both similar and nonsimilar problems. The dynamic viscosity μ and the Prandtl number, which is a function of viscosity, have been considered variable during the solution procedure. A detailed description of the solution procedure, with variable thermophysical properties, may be found in [9].

3. Results and discussion

The governing parameters of this problem is the viscosity parameter A, the Hartmann number M and the similarity variable η defined as [1]

$$A = b(T_w - T_a) \tag{8}$$

$$\frac{\sigma B_0^2}{\rho} = cM^2 \tag{9}$$

$$\eta = v_a^{-1/2} c^{1/2} y = \frac{y}{x} Re_x^{1/2} \tag{10}$$

where v_a is the ambient fluid kinematic viscosity and Re_x is local Reynolds number defined as

$$Re_x = \frac{u_w x}{v_a} \tag{11}$$

It should be noted here that when $A = 0$ the fluid viscosity is constant.

Mukhopadhyay et al. [1] transformed Eqs. (1)–(3) into the following ordinary differential equations:

$$f'^2 - ff'' = -A\theta' f'' + (a + A - A\theta) f''' - M^2 f' \tag{12}$$

$$\theta'' + Prf\theta' = 0 \tag{13}$$

where θ is the dimensionless temperature

$$\theta(\eta) = \frac{T - T_a}{T_w - T_a} \tag{14}$$

and f' is the dimensionless velocity

$$f'(\eta) = \frac{u}{u_w} \tag{15}$$

In the transformed energy equation (13) the Prandtl number appears. Mukhopadhyay et al. [1] solved Eqs. (12) and (13) considering the Prandtl number constant and equal to ambient Prandtl number given by the following equation:

$$Pr_a = \frac{v_a}{\kappa} \tag{16}$$

However, the Prandtl number is a function of viscosity and as viscosity varies across the boundary layer, the Prandtl number varies, too (see Fig. 10). For example the Prandtl number at the plate surface is

$$Pr_w = \frac{v_w}{\kappa} \tag{17}$$

This disadvantage will be discussed later.

In order to test the accuracy of our method, results were compared with those available in the literature. The wall heat transfer $\theta'(0)$ and the wall shear stress $f''(0)$ defined as

$$\theta'(0) = \frac{x}{T_w - T_a} (Re_x)^{-1/2} \left[\frac{\partial T}{\partial y}\right]_{y=0} \tag{18}$$

$$f''(0) = \frac{\mu_w}{\rho u_w^2} (Re_x)^{1/2} \left[\frac{\partial u}{\partial y}\right]_{y=0} \tag{19}$$

are shown in Table 1. The comparison is satisfactory.

It should be noted that for the case $A = 0$ (constant viscosity) and $M = 0$ there are analytical solutions for the velocity and temperature profiles. The velocity profiles are given by Gupta and Gupta [13]

$$f'(\eta) = e^{-\eta} \tag{20}$$

and are independent of the Prandtl number. The temperature profiles are given by Chiam [10]

$$\theta(\eta) = 1 - \frac{\int_0^\eta \exp[-Pr(\xi + e^{-\xi})]d\xi}{\int_0^\infty \exp[-Pr(\xi + e^{-\xi})]d\xi} \tag{21}$$

Table 1
Comparison of the present method results with those existing in the literature for $A = 0$ (constant viscosity)

Pr	$\theta'(0)$				$f''(0)$			
	Chiam [10]	Carragher and Crane [11]	Grubka and Bobba [12]	Present method	Chiam [10]	Carragher and Crane [11]	Grubka and Bobba [12]	Present method
0.023	−0.022489			−0.0240				−1.0050
0.10	−0.091292			−0.0925				−1.0050
1.0	−0.581977			−0.5820				−1.0050
0.7		−0.46		−0.4543		−1.0		−1.0050
10.0			−2.3080	−2.3080			−1.0	−1.0050

The following figures correspond to those presented by Mukhopadhyay et al. [1] (with the same captions) where we included our results and some analytical solutions. In Fig. 2 velocity profiles are shown for $Pr_a = 0.1$, $M = 0$ and two values of the viscosity parameter A. At the same figure the analytical solution is shown for $A = 0$. The velocity profile of our method for $A = 0$ is identical with the analytical solution and this is another proof that our method gives accurate results. It is also seen that the profiles of our method and those by Mukhopadhyay et al. [1] compare well and the same happens with the velocity profiles shown in Fig. 4. In Figs. 3, 5, 6 and 7 temperature profiles are shown for different values of Pr_a, M and A. In Figs. 3, 5 and 7 the temperature profiles derived by the analytical solution of Chiam [10] for $A = 0$ and $M = 0$ have been also included. We see that our temperature profiles compare

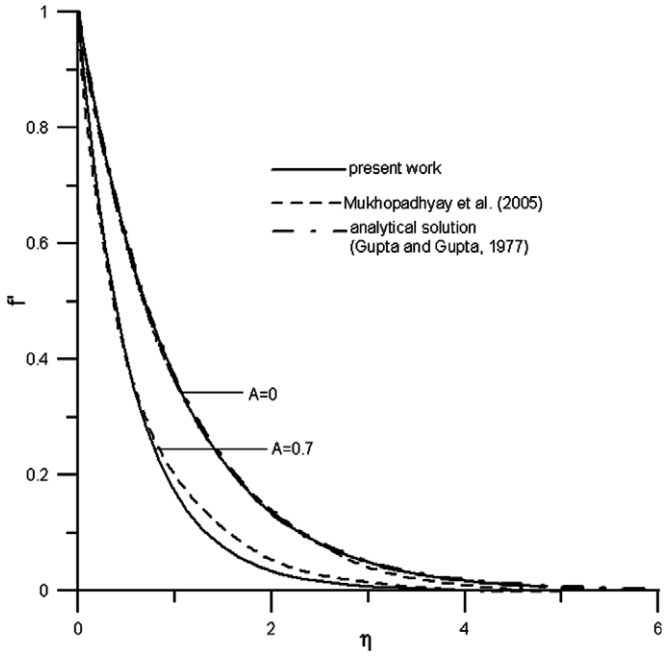

Fig. 2. Distribution of velocity against n when $M = 0$ and $Pr_a = 0.1$: solid line, present work: dashed line, [1].

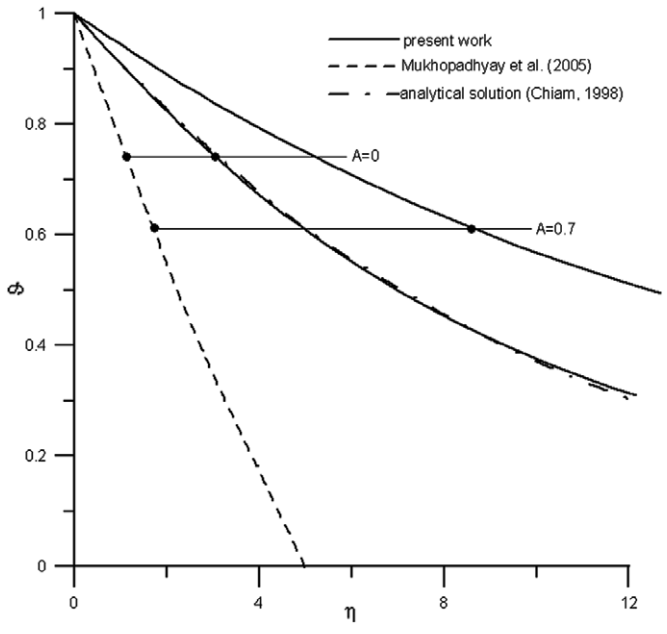

Fig. 3. Distribution of temperature against n when $M = 0$ and $Pr_a = 0.1$: solid line, present work: dashed line, [1].

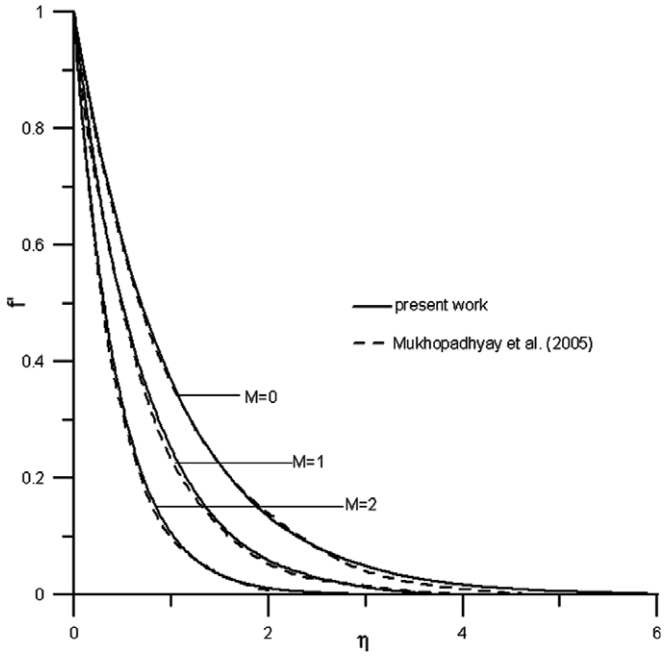

Fig. 4. Distribution of velocity against n when $A = 0$ and $Pr_a = 0.1$: solid line, present work: dashed line, [1].

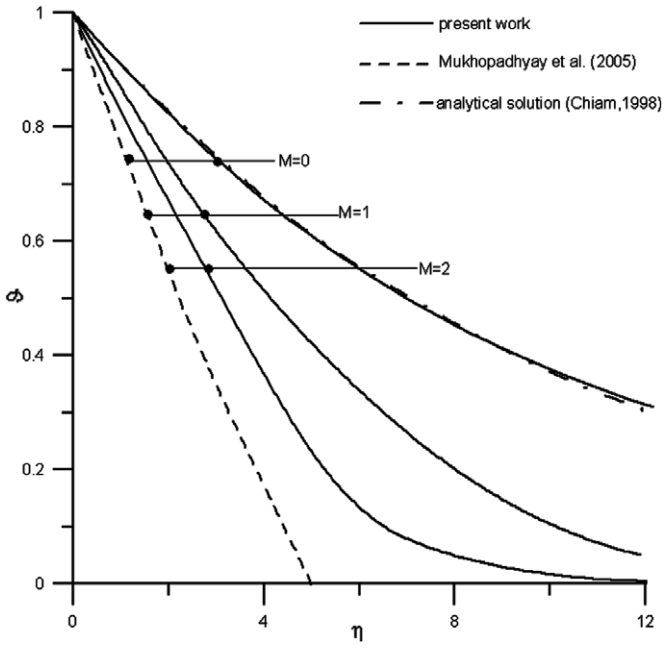

Fig. 5. Distribution of temperature against n when $A = 0$ and $Pr_a = 0.1$: solid line, present work: dashed line, [1].

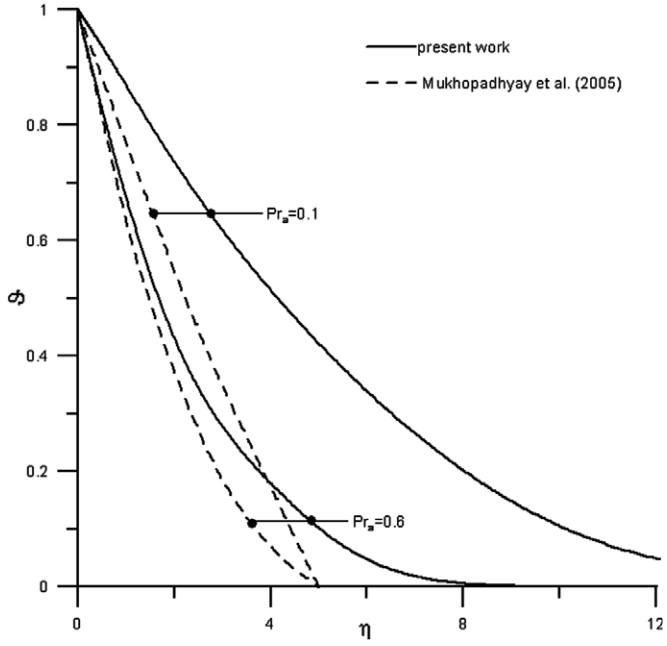

Fig. 6. Distribution of temperature against n when $A = 0$ and $M = 1$: solid line, present work: dashed line, [1].

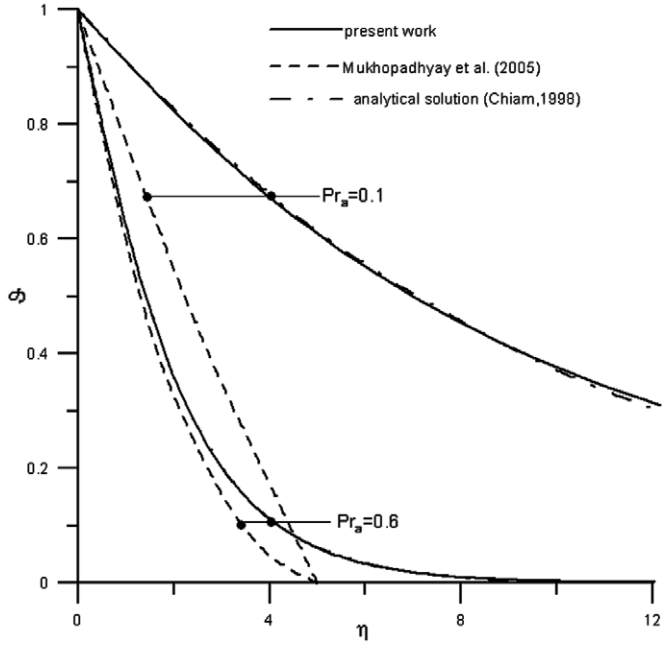

Fig. 7. Distribution of temperature against n when $A = 0$ and $M = 0$: solid line, present work: dashed line, [1].

very well with the profiles of the analytical solution. However large differences exist between our profiles and those of Mukhopadhyay et al. [1]. It is seen that the real temperature profiles, calculated by the present method, are much wider than those calculated by Mukhopadhyay et al. [1]. It is obvious that the temperature profiles by Mukhopadhyay et al. [1] are truncated due to a small calculation domain used. Apparently the authors used a calculation domain ($\eta_{\max}$) that is much smaller than the temperature boundary layer thickness. It is well known in the boundary layer theory that large Prandtl numbers correspond to thin temperature profiles and small Prandtl numbers to wider temperature profiles. The calculation domain that they used was sufficient to capture the velocity profiles but insufficient to capture the temperature profiles for this small Prandtl number (0.1). Chiam [10], in order to get accurate results for the same Prandtl number (0.1), used a calculation domain equal to 165 which is 33 times larger than that used by Mukhopadhyay et al. ($\eta_{\max} = 5$). Very large values of η have been used also in the present work to capture the very wide temperature profiles. The omission of Mukhopadhyay et al. to compare their results with those existing in the literature led to this disadvantage.

As was mentioned before the second disadvantage of the published work is the assumption that the Prandtl number is constant in the energy equation and equal to ambient Prandtl number. This is a wrong assumption. For example the dependence of Pr number on temperature for air is given by the following equation [14]:

$$Pr = 1.0677 \times 10^{-23} T^7 - 7.6511 \times 10^{-20} T^6 + 1.0395 \times 10^{-16} T^5 + 4.6851 \times 10^{-13} T^4 - 1.7698 \times 10^{-9} T^3 + 2.2260 \times 10^{-6} T^2 - 1.1262 \times 10^{-3} T + 0.88353 \quad \text{for} \quad 100\,K < T < 3000\,K) \tag{22}$$

For water the Pr number depends on temperature according to the following equation [15]:

$$Pr = 13.66/(7.4779458t^4 - 68.8626188t^3 + 197.7604676t^2 - 208.7474538t + 73.376906) \tag{23}$$

where $t = T/273.16$ and $273.16 < T < 373.16$ K. The above equations have been derived taking into account the variation of all fluid properties (μ, k, c_p) with temperature. The variation of air and water Pr number with temperature is shown in Figs. 8 and 9, respectively.

Mukhopadhyay et al. [1] used a hypothetical fluid whose viscosity μ is a linear function of temperature (Eq. (6)) and the other fluid properties constant. For this hypothetical fluid the variation of Pr number inside the boundary layer is shown in Fig. 10. The real Pr number (solid line) has been calculated as follows: We solved directly Eqs. (1)–(3) using the finite difference method of Patankar and we calculated the velocities and temperatures across the boundary layer for $Pr_a = 1$. Knowing the temperature across the boundary layer we calculated the viscosity μ from Eq. (6) and the Pr number from $Pr = \mu/\rho\kappa$ (ρ and κ constant). It is seen that the real Pr number is much smaller than the ambient one. Turning now to Fig. 3 we see that the temperature profiles by Mukhopadhyay et al. [1] for $A = 0$ and $A = 0.7$ are almost identical whereas the corresponding profiles of the present work differ significantly. Our profile for $A = 0.7$ is much thicker than that of $A = 0$ because in our method both viscosity and Prandtl

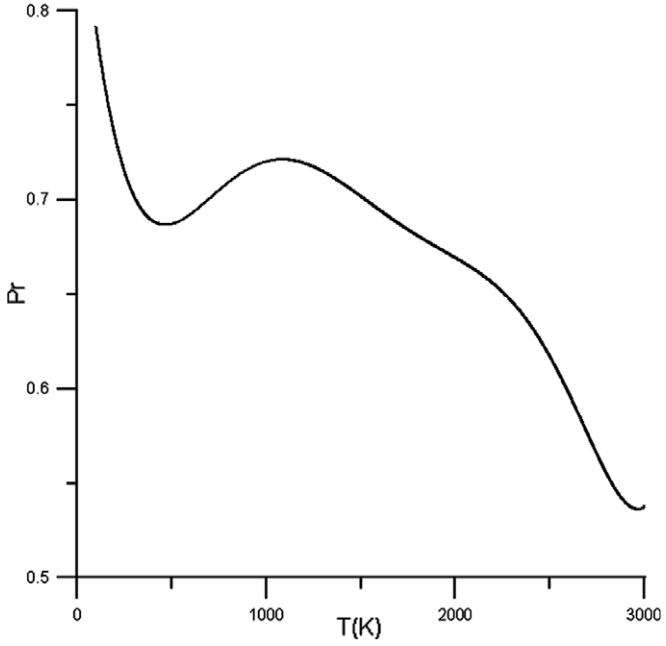

Fig. 8. Variation of air Prandtl number with temperature.

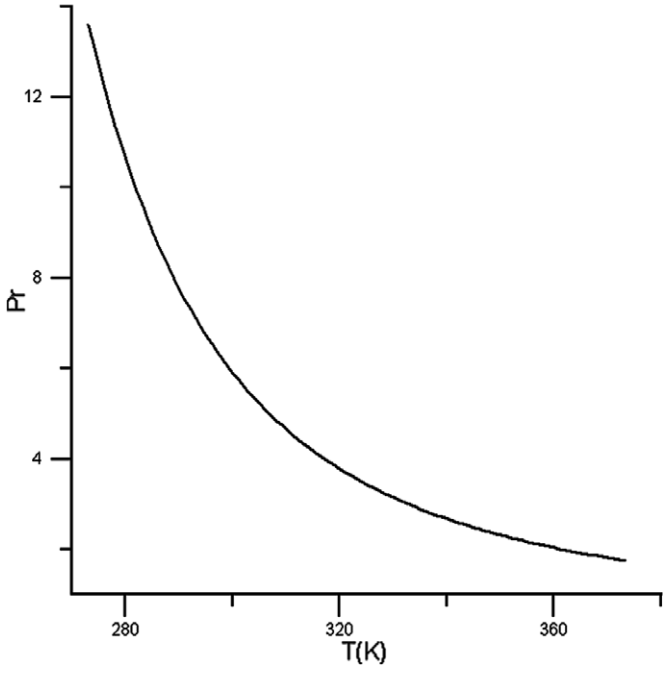

Fig. 9. Variation of water Prandtl number with temperature.

number are considered variable inside the boundary layer. The real Prandtl number near the plate is small and this leads to a wider temperature profile according to the boundary layer theory (large Prandtl numbers correspond to thin temperature profiles and small Prandtl numbers correspond to wider temperature profiles). It is difficult to find out the real reason that the two temperature profiles by Mukhopadhyay et al. [1] are identical because both profiles have been truncated. However the assumption of constant Prandtl number in the energy equation may lead to severe errors, especially when the variation of viscosity with temperature is strong, as was pointed out by Pantokratoras in three recent papers [16–18].

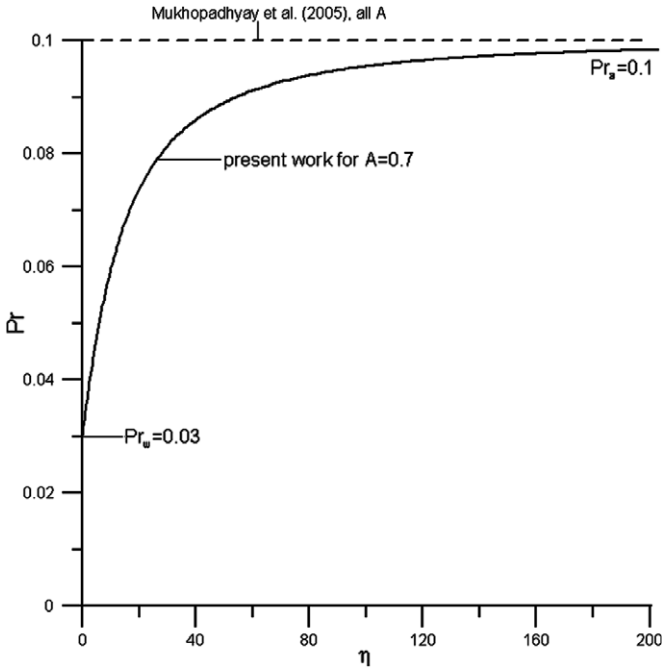

Fig. 10. Variation of Prandtl number across the boundary layer for $Pr_a = 0.1$: solid line, present work: dashed line, [1].

References

[1] S. Mukhopadhyay, G.C. Layek, Sk.A. Samad, Study of MHD boundary layer flow over a heated stretching sheet with variable viscosity, Int. J. Heat Mass Transfer 48 (2005) 4460–4466.
[2] B.C. Sakiadis, Boundary layer behavior on continuous solid surfaces: The boundary layer on a continuous flat surface, AIChE J. 7 (1961) 221–225.
[3] S.V. Patankar, Numerical Heat Transfer and Fluid Flow, McGraw-Hill Book Company, New York, 1980.
[4] R. Cortell, A note on flow and heat transfer of a viscoelastic fluid over a stretching sheet, Int. J. Non-Linear Mech. 41 (2006) 78–85.
[5] R. Cortell, Flow and heat transfer of an electrically conducting fluid of second grade over a stretching sheet subject to suction and to a transverse magnetic field, Int. J. Heat Mass Transfer 49 (2006) 1851–1856.
[6] S.V. Patankar, D.B. Spalding, Heat and Mass Transfer in Boundary Layers, Intertext, London, 1970.
[7] F. White, Viscous Fluid Flow, McGraw-Hill, New York, 1991.
[8] D. Anderson, J. Tannehill, R. Pletcher, Computational Fluid Mechanics and Heat Transfer, McGraw-Hill Book Company, New York, 1984.
[9] A. Pantokratoras, Laminar free-convection over a vertical plate with uniform blowing or suction in water with variable physical properties, Int. J. Heat Mass Transfer 45 (2002) 963–977.
[10] T.C. Chiam, Heat transfer in a fluid with variable thermal conductivity over a linearly stretching sheet, Acta Mech. 129 (1998) 63–72.
[11] P. Carragher, L.J. Crane, Heat transfer on a continuous stretching sheet, ZAMM 62 (1982) 564–565.

[12] L.J. Grubka, K.M. Bobba, Heat transfer characteristics of a continuous stretching surface with variable temperature, ASME J. Heat Transfer 107 (1985) 248–250.
[13] P.S. Gupta, A.S. Gupta, Heat and mass transfer on a stretching sheet with suction or blowing, Can. J. Chem. Eng. 55 (1977) 744–746.
[14] A.I. Zografos, W.A. Martin, J.E. Sunderland, Equations of properties as a function of temperature for seven fluids, Comput. Meth. Appl. Mech. Eng. 61 (1987) 177–187.
[15] T. Cebeci, J. Cousteix, Modeling and Computation of Boundary-Layer Flows, Horizons Publishing Inc., Long Beach, 1999.
[16] A. Pantokratoras, Further results on the variable viscosity on flow and heat transfer to a continuous moving flat plate, Int. J. Eng. Sci. 42 (2004) 1891–1896.
[17] A. Pantokratoras, Forced and mixed convection boundary layer flow along a flat plate with variable viscosity and variable Prandtl number: new results, Heat Mass Transfer 41 (2005) 1085–1094.
[18] A. Pantokratoras, Non-Darcian forced convection heat transfer over a flat plate in a porous medium with variable viscosity and variable Prandtl number, J. Porous Media 10 (2007) 201–208.